Toward Peltier-cooled mid-infrared HgCdTe lasers: Analyzing the temperature quenching of stimulated emission at ∼6 μ m wavelength from HgCdTe quantum wells

K. Kudryavtsev, V. Rumyantsev, V. Utochkin, M. Fadeev, V. Ya. Aleshkin, A. Dubinov, M. Zholudev, N. Mikhailov, S. Dvoretskii, V. Remesnik, et al.

Journal of Applied Physics

Toward Peltier-cooled mid-infrared HgCdTe lasers: Analyzing the temperature quenching of stimulated emission at ~6 μm wavelength from HgCdTe quantum wells

Cite as: J. Appl. Phys. **130**, 214302 (2021); https://doi.org/10.1063/5.0071908
Submitted: 17 September 2021 • Accepted: 13 November 2021 • Published Online: 02 December 2021

K. E. Kudryavtsev, V. V. Rumyantsev, V. V. Utochkin, et al.

AIP Publishing

Journal of Applied Physics ARTICLE scitation.org/journal/jap

Toward Peltier-cooled mid-infrared HgCdTe lasers: Analyzing the temperature quenching of stimulated emission at ~6 μm wavelength from HgCdTe quantum wells

Cite as: J. Appl. Phys. **130**, 214302 (2021); doi: 10.1063/5.0071908
Submitted: 17 September 2021 · Accepted: 13 November 2021 ·
Published Online: 2 December 2021

K. E. Kudryavtsev,[1,2,a)] V. V. Rumyantsev,[1] V. V. Utochkin,[1] M. A. Fadeev,[1] V. Ya. Aleshkin,[1] A. A. Dubinov,[1] M. S. Zholudev,[1] N. N. Mikhailov,[3] S. A. Dvoretskii,[3] V. G. Remesnik,[3] F. Teppe,[4] V. I. Gavrilenko,[1] and S. V. Morozov[1,2]

AFFILIATIONS

[1]Institute for Physics of Microstructures, Russian Academy of Sciences, 603087 Nizhniy Novgorod, Russia
[2]Faculty of Radiophysics, Lobachevsky University of Nizhny Novgorod, 603950 Nizhny Novgorod, Russia
[3]Institute of Semiconductor Physics, Siberian Branch of Russian Academy of Sciences, 13 Lavrentiev Ave., 630090 Novosibirsk, Russia
[4]Université de Montpellier, Laboratoire Charles Coulumb, F-34095 Montpellier, France

[a)]**Author to whom correspondence should be addressed:** konstantin@ipmras.ru

ABSTRACT

Despite the ultimate performance of the existing cascade lasers, simple interband emitters in the mid-infrared (IR) can still be of interest as a cheaper and widely tunable alternative for some applications. In this work, we show mid-infrared stimulated emission (SE) at 5–6 μm wavelength from an optically pumped mercury–cadmium–telluride quantum well (QW) heterostructures at temperatures up to 200 K. At lower temperatures, the SE threshold appears to be mostly determined by conventional *eeh* Auger recombination, while the contribution of alternative QW-specific *ehh* Auger processes is limited. At higher temperatures, we establish heating of the electron gas by pumping radiation as a primary factor responsible for the thermal quenching of the SE. Consequently, both pumping scheme and QW designs should be carefully revised to minimize carrier heating in order to realize near-to-mid-IR optical converters operating close to ambient temperature. We suggest using low-barrier QWs to minimize excessive heat introduced in the QW upon carrier capture and also to eliminate *eeh* Auger processes involving excited QW subbands. Thus, mid-infrared HgCdTe lasers are expected to reach operating temperatures readily attainable under thermoelectric cooling.

I. INTRODUCTION

Mercury–cadmium–telluride (HgCdTe) is a well established system in infrared (IR) photonics serving as a detector material throughout the entire range from near- to far-IR.[1,2] While HgCdTe-based structures are also considered as light emitters, their performance may be severely limited by strong non-radiative recombination via the Auger mechanism typical for narrow-gap semiconductors (see Ref. 3 and references within). At the same time, Auger processes could be substantially suppressed provided that the electron and hole dispersion laws impose substantial activation energy for these processes, which is required to fulfill momentum and energy conservation.[4] For parabolic bands, the Auger threshold approaches half the bandgap energy in case of symmetric dispersion with nearly equal electron and hole masses. Somewhat similar band dispersion symmetrical in the vicinity of the Γ-point of the Brillouin zone may be realized in HgTe/CdHgTe quantum well (QW) heterostructures,[5,6] allowing to obtain stimulated emission (SE) up to 20 μm.[7] Yet, long-wavelength lasing from HgCdTe seems possible at cryogenic temperatures only, and so, mostly represents scientific interest. Likewise, the near-infrared

range at 1.5–2.5 μm is not exactly the domain of practical HgCdTe lasers (despite numerous works on room-temperature lasing from both bulk HgCdTe[8–10] and QW heterostructures),[11,12] since this range is readily accessible by available III–V emitters.[13,14] However, at intermediate wavelengths (~3–10 μm), HgCdTe-based QWs appear promising as a laser material being only opposed by cascade and lead salt[15] lasers. Whereas, cascade lasers provide exceptional output characteristics and serve as an indisputable benchmark in the field,[14,16–17] HgCdTe lasers (either diode lasers or optical converters) might offer cost-efficient solutions complementing cascade lasers as mid-IR light sources in certain applications.[18] With lasing temperatures in excess of 170–200 K achieved at wavelengths as long as 10 μm,[19–21] thermoelectric-cooled operation of future HgCdTe QW based lasers at shorter wavelengths (~3–6 μm) seems quite feasible. Indeed, operating temperatures up to 200 K at 5–6 μm, demonstrated in this work, show a considerable improvement over the values achieved in early works (~60 K in Ref. 22)and suggest that the entire atmosphere transparency window at 3–5 μm can be covered with thermoelectric cooling.

A comprehensive understanding of carrier dynamics is essential to improve the performance of mid-IR HgTe/CdHgTe QW lasers toward the practical level. At the same time, studies of interband processes (and in particular, Auger recombination) are only extensive for bulk HgCdTe (e.g., Refs. 23–25). Still, most works deal with relatively low carrier concentrations (few exceptions are Refs. 23 and 26) typical for photodetectors, but not relevant to lasing. Considering HgCdTe QW heterostructures, experimental data are even more limited and generally refer to the QWs designed for long-wavelength emission.[20,27,28] For mid-IR QWs, *eeh*-type AR was evaluated indirectly for QWs emitting around 3 μm,[29] and at longer wavelengths, the picture becomes more complicated since the fundamental bandgap energy is comparable to the intersubband spacing in the QW. Thus, several additional factors may come into play, including resonant (non-threshold) Auger processes with interband recombination energy directed to heat third particle into the excited QW subband[30] and intervalence free-carrier absorption.[31] While both were marked in many preceding works,[32–34] only brief theoretical estimates were provided with no detailed discussion and no experiment following. The latter is perfectly explainable seeing that molecular beam epitaxy (MBE) growth of high-quality few-nanometer-thick HgTe/CdHeTe QWs suggested in Ref. 33 was not mastered until quite recently.[35,36] Following the advances in growth technology, the practical potential of HgTe/CdHgTe QWs has to be re-evaluated, and resonant Auger processes were analyzed in more detail in Ref. 37; however, attention was mostly focused on a very narrow gap, far-IR QWs, and the work cited is still purely theoretical. In the present paper, we study temperature quenching of mid-infrared ($\lambda \sim 5$–6 μm at $T \sim 200$ K) stimulated emission from HgTe/CdHeTe QW heterostructures in an attempt to identify individual contributions of different Auger processes into interband carrier dynamics and to determine mechanisms limiting maximum lasing temperature for optically pumped structures.

II. SAMPLES AND EXPERIMENT

Investigated samples were MBE grown on (013)GaAs substrates with CdTe/ZnTe buffer layers. The design of the active region was generally similar to those reported in Ref. 19, with 10 HgTe (nominally binary) QWs, 4.3-nm thick and separated by 30-nm thick $Cd_{0.6}Hg_{0.4}Te$ barriers. Waveguide (optical confinement) layer was also 60%-cadmium CdHgTe with a total thickness of 5.2 μm. The active region was capped by a 50-nm CdTe layer. *In situ* ellipsometry data and post-growth sample characterization by photoluminescence (PL) and photoconductivity confirmed the composition of barrier layer at $x[\mathrm{Cd}]_{\mathrm{barr}} \sim 60\%$, while the residual cadmium content in the QWs (x[Cd]) varied slightly throughout the series. For three samples studied, the values x[Cd] = 7%, 8.5%, and 10.5%, respectively, were determined, corresponding to the emission wavelengths of 5.9, 5.3, and 4.9 μm at $T = 200$ K (8.1, 6.6, and 5.9 μm at liquid helium temperature). Since all three samples demonstrate very similar behavior, we will focus our discussion on the most narrow-gap sample with 7% residual [Cd], further in this work. Given the above QW parameters, the electronic band structure in the QW was calculated within a four-band $\mathbf{k}\cdot\mathbf{p}$ Kane model with account to deformation effects according to Ref. 38, the model proved to be very consistent with experiment further in Ref. 39. Resulting electronic spectra are provided in Fig. 1, indicating also possible Auger recombination pathways: conventional *eeh* process [CCH-C, Fig. 1(a)], which may be considered "bulk-like" in terms that only fundamental electronic subbands (*e*1 and *h*1) are involved, and QW-specific *ehh* [CHH-H, Fig. 1(b)] and *eeh* [CCH-C2, Fig. 1(c)] processes that also involve excited QW subbands to host the resulting energetic particle.

For PL and SE studies, we used a Bruker Vertex80v Fourier-transform spectrometer equipped with liquid nitrogen cooled mercury–cadmium telluride photodetector (16 μm cut-off wavelength) and operating in the step-scan mode. Investigated samples

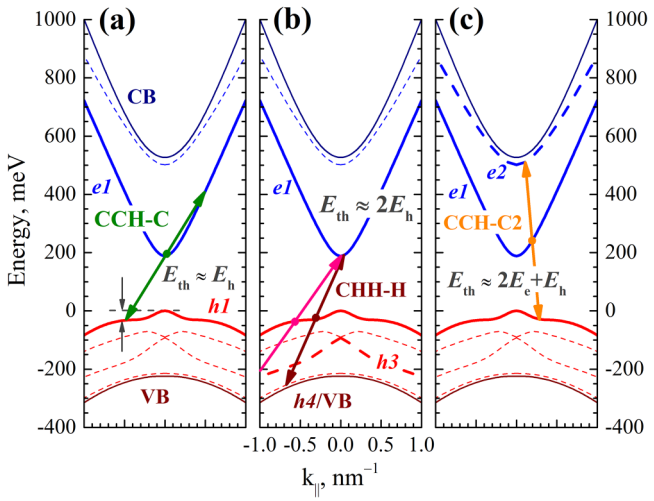

FIG. 1. Calculated band dispersion for 4.3 nm thick Hg(Cd)Te/CdHgTe QWs with 7% residual [Cd] fraction in the QWs at $T = 180$ K. Arrows show a graphical depiction of possible Auger processes: conventional CCH-C (a), QW-specific CHH-H (b), and CCH-C2 (c) processes involving either excited states in the QW or continuum states above the barrier level. Energy thresholds for corresponding AR processes are also marked.

were mounted in a closed-cycle refrigerator allowing temperature-dependent measurements in the range of $T = 10$–320 K. For all luminescence studies, we used near-IR parametric optical oscillator emitting at 2.05 μm wavelength as an excitation source to realize below-barrier, direct pumping of the QWs ensuring uniform and predictable excitation of all the QWs in the array; and stray pump light was filtered out by an InAs plate.

III. RESULTS AND DISCUSSION

For the evaluation of non-radiative processes in HgTe/CdHgTe QWs, direct measurement of interband carrier dynamics (for example, via photoconductivity kinetics studies[20]) should be an ideal approach to rely on. It is, however, tricky to perform for relatively wide-gap QWs under consideration, given both nanosecond-scale temporal resolution of our setup (limited by the duration of excitation pulses $\tau_{pump} \sim 10$ ns) and rather fast (~50 ns) radiative recombination, leaving only a tiny rate window of 10–50 ns for non-radiative recombination to manifest itself. Alternatively, indirect estimates for carrier lifetime may be provided based on measured stimulated emission threshold using a simple relation,

$$\tau_{eff} = \frac{n_{th}}{\alpha_{QW} G_{th}}, \quad (1)$$

where n_{th} and G_{th} are excess carrier concentration and incoming photon flux corresponding to the SE threshold intensity, respectively, and α is the light absorption factor of the QWs for direct (below-barrier) pumping which is typically $\alpha \approx 0.01$. By using Eq. (1), we assume a quasi-steady-state regime within the excitation pulse so that $t_{eff} \ll t_{pump}$. Another important point is that we consider threshold concentration n_{th} equal to the QW transparency concentration N_{inv} which seems reasonable for mid-IR HgTe/CdHgTe QWs under study. With lattice-related absorption ruled out due to relatively short-wavelength emission at $\lambda < 6$–8 μm (while obviously contributing to waveguide losses at longer wavelengths),[40] free-carrier absorption (FCA) also appears to be of minor importance. Both our estimates and data fromRef. 37 suggest that a nearly imperceptible increase in threshold concentration n_{th} (no more than 5% of the interband transparency concentration N_{inv} under the worst conditions) is sufficient to compensate for the FCA. Thus, with no efficient mechanism for internal optical losses, SE onset is expected just after QW interband transparency is achieved.

In Fig. 2, we show measured SE threshold intensities depending on sample temperature alongside calculated QW transparency concentrations N_{inv} for the QWs under study. For calculation of N_{inv}, effective carrier temperature was taken equal to lattice temperature. Note that calculated QW transparency concentrations are nearly identical for all samples in the series at any given temperature, and measured SE thresholds are also similar within 15%–20% intervals. One can see from Fig. 2 that the SE threshold increases faster with temperature than N_{inv}, which supposedly indicates thermal activation of non-radiative processes. At $T = 90$ K, we estimate $\tau_{eff} \sim 1$ ns, which is definitely Auger-limited, since given τ_{eff} is much faster than calculated radiative lifetime (>10 ns), and thus, our "steady-state" approximation is justified at relevant temperatures ($T > 90$ K). We do not discuss lower temperatures in order to avoid the case of $\tau_{eff} \geq \tau_{pump}$; such a relation would lead to a complicated carrier dynamics with initial inversion "build-up" during a certain fraction of the excitation pulse before SE occurs.

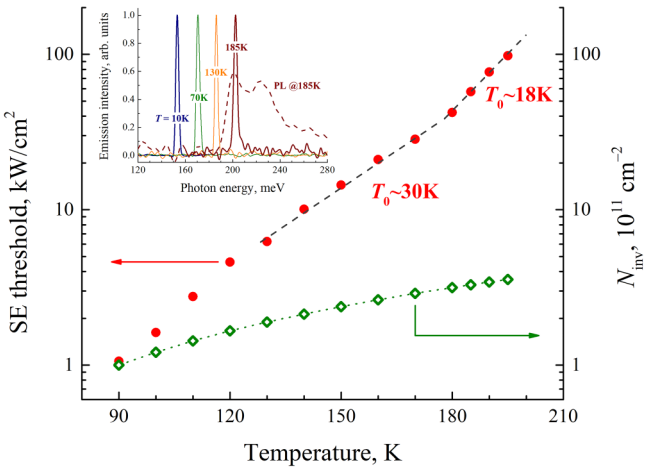

FIG. 2. Solid circles: measured SE threshold depending on sample temperature; and characteristic temperatures corresponding to low- and high-temperature regions are marked. Open diamonds: calculated SE threshold (QW transparency) concentration, assuming electronic temperatures equal to lattice temperature. In the inset, normalized SE spectra measured at different sample temperatures; and for comparison, spontaneous emission spectra measured at $T = 185$ K just below the SE threshold are also presented.

A. Conventional (*eeh*) Auger recombination

Let us first refer to CCH-C type AR which only involves carriers in the fundamental electron and hole subbands in the QW according to Fig. 1(a). This process is expected to determine non-radiative rates in the QWs under study (at least at relatively low temperatures, before the resonant onset of competing zero-threshold processes). In Fig. 3, we show effective carrier lifetimes estimated from data in Fig. 1 using Eq. (1) depending on sample temperature with two distinct regions separated by a visible break around $T \sim 180$ K. In fact, at $T < 180$ K, CCH-C AR appears to be the only candidate to define interband recombination rate under intense pumping close to the SE threshold. Though detailed microscopic calculations of AR rates (similar to presented in Refs. 37, 41, and 42) may be required to support this idea to the full extent, in this work, we consider a simple model to evaluate thermal activation of the CCH-C process. With two electrons and one hole participating in CCH-C AR, a corresponding recombination rate may be expressed as

$$R_{CCH-C} = C_A \times n_{act}^2 \times h_{act}. \quad (2)$$

Here C is a constant, temperature-independent microscopic Auger coefficient, while n_{act} and h_{act} are concentrations of "active" electrons and holes, which possess sufficient kinetic energies to overcome the AR energy threshold—certain minimal kinetic energy of the initial e–e–h system required to fulfill energy-momentum

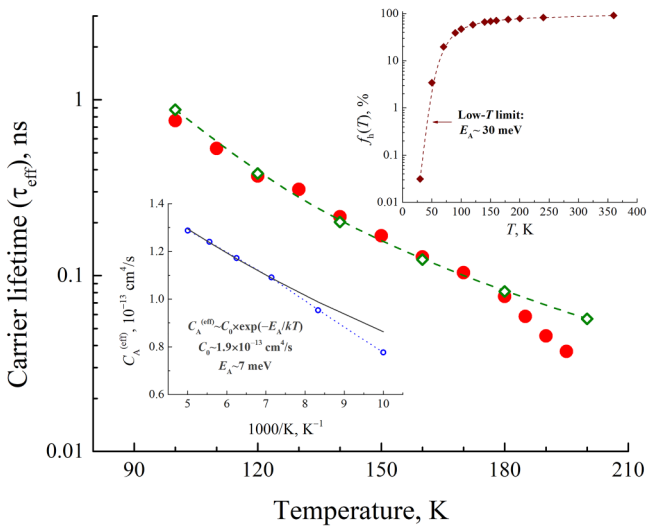

FIG. 3. Estimated carrier lifetimes at SE threshold depending on temperature: (solid circles) calculated from the experiment; (open diamonds): model fit for Auger-1 CCH-C process according to Eq. (3). In the insets, (top right) $f_h(T)$ plot showing the fraction of above-threshold holes; note that apparent "activation energy" (derived from the exponential fit) corresponds to calculated "Auger threshold" energy (~27 meV) only at temperatures below that of liquid nitrogen; and (bottom left): temperature activation of Auger recombination within T = 100–200 K.

conservation. This energy threshold, calculated according to Ref. 43, amounts to $E_{th} \sim 26$–27 meV for the samples studied, and the most important point for the *eeh* Auger process is that this threshold energy is carried almost completely by the hole [as it may be deduced from the graphical depiction of CCH-C AR in Fig. 1(a)]. Thus, virtually all electrons in the QW are above threshold with respect to AR and so we assume $n_{act} = N_{inv}$ in Eq. (2). This is not the case for the holes; and due to substantial E_{th} value (higher than the thermal energy kT at relevant temperatures), only a fraction of (energetic) holes is actually "Auger-active," and h_{act} does not simply follow N_{inv}. Based on the hole dispersion law and taking Fermi–Dirac statistics, we calculate the fraction of above-threshold holes with kinetic energies exceeding E_{th}. Defined further as $f_h(T) \equiv h_{act}(T)/N_{inv}(T)$, this quantity is plotted in the inset in Fig. 3. Finally, Eq. (2) can be written in the following form:

$$R_{CCH\text{-}C}(T) = C_A \times N_{inv}^3(T) \times f_h(T), \tag{2a}$$

$$\tau_{Aug}^{-1}(T) = C_A \times N_{inv}^2 \times f_h(T). \tag{3}$$

In Fig. 3, Eq. (3) provides a good model fit to the experimental data in Fig. 2 while only using a single fitting parameter, $C = 2.7 \times 10^{-13}$ cm^4/s. Interestingly, if one defines temperature-dependent, *apparent* Auger coefficient $C^{(eff)}$ according to $R_{CCH\text{-}C} = C_A^{(eff)} \times N_{inv}^3$, we observe a rather weak activation of the AR between $T \sim 90$ and ~170 K. Given in the inset in Fig. 3, corresponding $C_A^{(eff)}(T)$ dependence is close to the exponential function with a characteristic energy E_A of just ~7–10 meV, much lower than calculated threshold energy for CCH-C process (~27 meV). This fact is directly related to strongly non-parabolic hole dispersion: pronounced "shoulders" away from the Γ-point lead to a strong peak in the hole density of states at corresponding energies, and so the fraction of "above-threshold" holes (with respect to the total hole concentration, n_{th}) is weakly dependent on temperature for $T > 80$–100 K (see the insets in Fig. 3). At the same time, for $T = 77$ K, we have $C_A^{(eff)} \sim 6 \times 10^{-14}$ cm^4/s, which is very close to theoretical predictions provided in Ref. 37 for binary HgTe/CdHgTe QWs, and room-temperature $C_A^{(eff)}$ estimate agrees reasonably with (extrapolated) experimental data on the bandgap dependence of Auger coefficients in various type-I QWs summarized in Ref. 3. Note also that the energy threshold for *eeh* Auger process appeared to be very similar for all three samples studied ($E_{th} \sim 26$–27 meV with the effect of the increasing bandgap countered by the increase in residual [Cd] content in the QWs); and alongside with close N_{inv} values, it explains a similar performance of these samples in terms of SE threshold.

The agreement between the temperature behavior of experimental and model estimates for the interband recombination rate presented in Fig. 3 indicates that the suggested "Auger threshold" model is plausible. However, at $T > 180$ K, a distinct break appears in the measured $P_{th}(T)$ curve [and so in calculated $\tau_{eff}(T)$ dependence, see Figs. 1 and 2, respectively] and our model deviates from the experiment, suggesting that it is not entirely CCH-C AR responsible for the temperature quenching of the SE. In Sec. III B, we will discuss competing, QW-specific mechanisms contributing to the effect.

B. Role of the QW-specific processes

In contrast to bulk HgCdTe, QW based heterostructures provide a rather complicated background for the analysis of electronic transitions and interband recombination. For mid-IR emitters, the presence of multiple excited states in the QWs, at least in the valence band, with energy spacing comparable to the fundamental bandgap potentially gives rise to many alternative Auger processes [see Fig. 1(b)]. To arrange these processes according to their expected relevance, we show in Fig. 4 calculated Auger threshold energies for CHH-H recombination (compared to CCH-C) depending on temperature. Here we only consider CHH-H processes resulting in the heating of the hole into higher QW subbands, $h3$ or $h4$, since processes resulting into $h1$ or $h2$ subband feature unrealistic energy thresholds in excess of 160–200 meV.

From Fig. 4, we consider resonant CHH-$H_{1\to4}$ processes (resulting in a hole being heated into the $h4$ subband) the most interesting; and for this process, calculated Auger threshold gradually decreases with temperature, overtaking the CCH-C process at $T \sim 180$ K and ultimately reaching $E_{th} = 0$ around $T = 240$ K. At this point, CHH-H AR may be depicted as purely vertical electronic transitions at $k = 0$ in Fig. 1(b). Comparing data in Figs. 2 and 4, one may suggest that a strong increase in the SE threshold power above $T = 180$ K is related to the onset of CHH-$H_{1\to4}$ recombination. In order to probe this resonant AR process experimentally, we measure integral emission intensity as a function of sample temperature (within $T = 160$–300 K range) under constant excitation power. Pump power (~10 kW/cm^2) was chosen to be below the SE

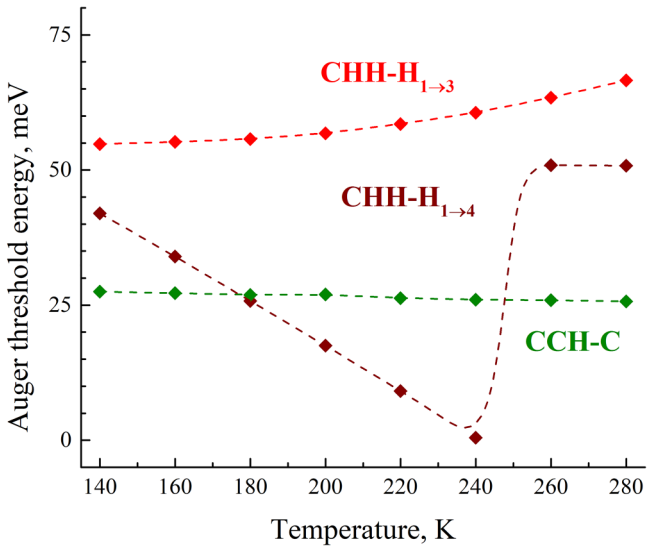

FIG. 4. Calculated threshold energies for competing CCH-C and CHH-H Auger processes depending on temperature.

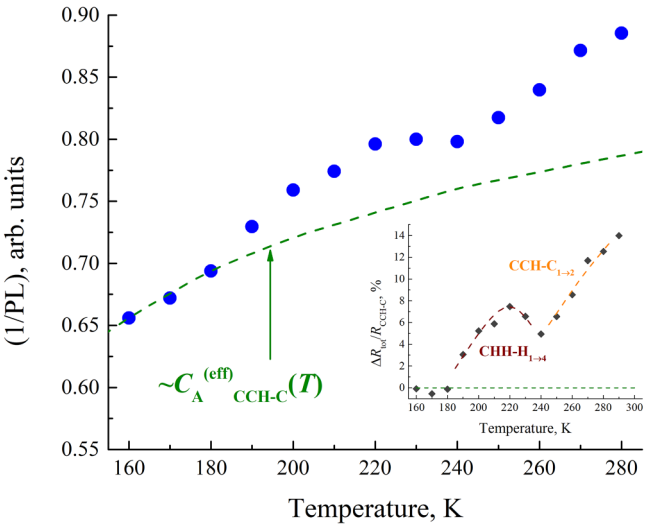

FIG. 5. Reciprocal integral PL intensity depending on the sample temperature for a fixed, below-threshold excitation power density (~10 kW/cm^2). Dashed line ($\sim C_A^{(eff)}{}_{CCH-C}$) represents thermal activation of the CCH-C Auger process. In the inset, estimates for the relative role of concurrent, QW-specific Auger processes (marked; dashed lines are guides to the eye) in the total "effective recombination rate" compared to the contribution of CCH-C recombination. Note that multiple experimental runs resulted in some 3% relative error between measured PL(T) curves.

threshold so that we only consider spontaneous light emission but still reasonably high to allow for the (i) saturation of possible SRH channels and (ii) dominant role of AR ($\tau_{Auger} \ll \tau_{rad}, \tau$). In this case, the PL intensity should generally follow the effective interband lifetime: $I \sim \tau_{eff}/\tau_{rad}$. Results are presented in Fig. 5.

Measured data are plotted as the PL^{-1} (T) dependence in Fig. 5 so that data points represent "effective recombination rate" ($1/\tau_{eff}$). As a reference, we also plot an estimated recombination rate for CCH-C only AR (dashed line), proportional to $C_A^{(eff)}(T)$ and extrapolated from our data in Fig. 3. The inset in Fig. 5 shows the relative difference between measured and reference curves so that the relative roles of competing Auger processes may be estimated. Here, we attribute two distinct regions (at $T = 180$–240 K and $T > 240$ K) to CHH-H$_{1\to4}$ and CCH-C$_{1\to2}$ [see Fig. 1(c) processes, respectively]. Our assumption is largely speculative regarding the latter process; and the increasing trend observed in ΔR_{tot} at higher temperatures may also be related to the decrease in radiative recombination rate since holes tend to be concentrated away from the Γ-point of the Brillouin zone at elevated temperatures. At the same time, the resonant feature observed at $T = 190$–230 K is what one might expect as a sign of CHH-H$_{1\to4}$ AR, given calculated Auger threshold energies from Fig. 4. However, the effect under consideration is rather weak with less than 10% variation of the carrier lifetime compared to the "non-resonant" background, suggesting that the dominant role of *eeh*-type Auger processes—even when competing *ehh*-type processes—have zero energy threshold.

Qualitatively, the prevalence of CCH-C processes may be explained by an unusual hole dispersion in the HgCdTe QWs under study featuring pronounced "shoulders" at $k \sim 0.3$–0.7 nm^{-1} (see Fig. 1). It results in a very high density of states at the energies corresponding to the plateau in the $h1$ dispersion ($E_{h0} \sim 30$ meV) compared to those at lower energies. Consequently, at relevant temperatures, the majority of excess holes belong to these side shoulders in the $h1$ subband with a typical distribution function of electrons and holes shown in Fig. 6. Thus, as the QW band structure is temperature-driven toward resonance at $T \sim 240$ K and electronic

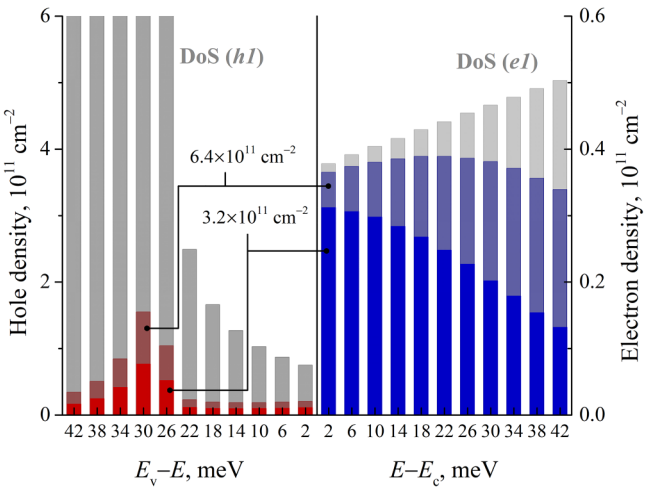

FIG. 6. Electron and hole distribution (given as 4-meV-wide bins) calculated at $T = 180$ K for excess carrier concentrations of $n = 3.2 \times 10^{11}$ cm^{-2} (which is the QW transparency concentration n_{th} at 180 K) and 6.4×10^{11} cm^{-2} ($2 \times n_{th}$). Gray bars represent the total density of states for $e1$ and $h1$ QW subbands.

transitions for CHH-$H_{1\to4}$ process tend to be closer to vertical, this process has to rely on the holes in the vicinity of $k = 0$, and only a tiny fraction of excess holes may actually participate in what is technically non-threshold Auger recombination. Note that, away from resonance electronic transitions for CHH-$H_{1\to4}$ process are diagonal [as it is shown in Fig. 1(b)] and one might, in fact, expect somewhat stronger CHH-H recombination since more holes could be involved. However, we suppose that "effective hole concentration" for *ehh* Auger processes remains relatively low compared to the total hole concentration. Indeed, taking a probe hole at $\boldsymbol{k} = \boldsymbol{k_0}$ belonging to the plateau in $h1$ dispersion ($|\boldsymbol{k_0}| \sim 0.3$–$0.7\ \mathrm{nm}^{-1}$), we so define the momentum being transferred to the second hole during AR process ($\Delta\boldsymbol{k_h} \approx \boldsymbol{k_0}$); and electrons can only provide a small correction here since they are tightly bunched around $k = 0$ in the k-space (with $|\boldsymbol{k_e}| < 0.1\ \mathrm{nm}^{-1}$). The energy being transferred to the resulting "hot" hole is also well determined: $\Delta E_h \approx E_g + E_{h0}$, with the tolerance given by the kinetic energy of the electron. These fixed $\Delta\boldsymbol{k_h}$ and ΔE_h values impose strong selection rules for the second (heated) hole completing three-particle *ehh* system considering that both initial and final states of this hole must fall into the hole dispersion branches ($h1$ and $h4$, respectively). Given the fact that holes are effectively spread in the k-space into a wide ring with $|\boldsymbol{k_0}| \sim 0.3$–$0.7\ \mathrm{nm}^{-1}$, only a certain, momentum-matched fraction of the total hole population satisfies this condition, thus suppressing CHH-H type Auger processes.

The same considerations may be applied for non-resonant CHH-$H_{1\to3}$ process (resulting in the $h3$ QW subband), which is also expected to be weak compared to CCH-C recombination due to the above-mentioned selection rules for participating holes, and not due to its high-energy threshold since both processes rely on the same particles—holes within the "shoulders" of the $h1$ subband—to cover the energy deficit for AR. For this reason, one might expect somewhat similar thermal activation for the Auger processes under discussion with individual contributions of either mechanism hardly distinguishable from temperature-dependent measurements. Thus, "Auger threshold energy" should be used with caution as a figure of merit while analyzing *ehh*-type Auger processes in HgCdTe-based QWs.

To conclude the discussion on CHH-H Auger recombination, we believe it to be of minor importance on the background of strong CCH-C processes. This idea is supported by the good fitting of our data in Fig. 2 using CCH-C only model. Note also that filling factors for holes are rather low (~0.1–0.2) throughout the entire distribution function at carrier concentrations close to the QW transparency point, and filling factors for electrons are close to unity. Thus, it appears intuitively sensible that Auger processes involving two holes (both CHH-$H_{1\to3}$ and CHH-$H_{1\to4}$ in Fig. 4) should generally be weaker than CCH-C with almost guaranteed two electrons at the bottom of the conduction band to recombine with an above-threshold hole. To be firmly sustained, these general considerations undoubtedly require both time-resolved experiments and extensive model computations, which are beyond the scope of the present paper. However, the experimental fact is that any resonant-like features are very slightly reflected in such a slow-rate process as PL, meaning that the corresponding impact on "fast" SE might be even smaller.

Finally, we should comment on the possible role of intervalence free-carrier absorption. Similar to electronic transitions during non-threshold AR, intervalence absorption may experience resonance at certain temperatures when optical transition energy in the QW ($e1 \to h1$ at $k = 0$) coincides with the energy of direct-k transitions between valence band states (here, $h1 \to h4$ at k-values corresponding to populated hole states at the plateau). While we do not have any experimental facts to evaluate the effect, our calculations show that light absorption due to $h1 \to h4$ transitions is orders of magnitude weaker than the characteristic scale of the optical gain. Furthermore, no SE could be obtained beyond 200 K (even after crossing all the band resonances at $T > 240$ K), so we consider factors other than Auger recombination and intervalence absorption responsible for observed quenching of the SE. The most likely of them is overheating of the electron gas.

C. The effect of carrier heating

While in preceding sections electronic temperatures were assumed equal to lattice temperature, it should only hold at sufficiently low pumping intensities. When it comes to stronger pumping required to achieve lasing at higher temperatures, carrier overheating becomes inevitable since (i) pump photons carry a lot of excess energy compared to the bandgap energy (~600 and ~200 meV, respectively) which has to be dissipated and (ii) carrier heating during Auger processes may become increasingly important. In order to evaluate this additional carrier heating, we derive effective electronic temperatures from the spontaneous emission spectra measured at a different excitation power by comparing the high-energy slope of the PL to the results of model calculations (see Fig. 7).

We do not observe visible effects up to $50\ \mathrm{kW/cm^2}$; and however, at stronger pumping, the estimated electronic temperature

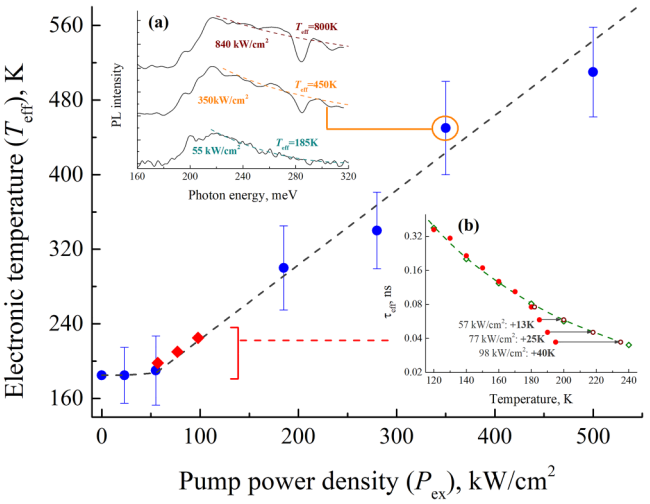

FIG. 7. Estimates for the carrier heating depending on the excitation power density with base (lattice) temperature $T_{latt} = 185$ K. In the insets, (a) PL spectra measured at different pump power (solid lines) and model curves representing estimated electronic temperatures (dashed lines) and (b) carrier heating estimated at SE threshold according to Eq. (3), assuming a single CCH-C recombination process.

starts to deviate from lattice temperature. Apart from direct measurements [inset (a) in Fig. 7], additional data may be recovered from the SE threshold measurements (see Figs. 2 and 3) assuming that it is carrier heating solely responsible for the increase in the SE threshold above 180 K: corresponding "projection" showing the difference between the sample and electronic temperatures is provided in the inset (b) in Fig. 7. Note that data from both direct and indirect measurements merge nicely in the resulting curve in Fig. 7. Given these data, our results on the temperature stability of the stimulated emission for the QWs under study are summarized in Fig. 8. The Solid line (T_{SE}^{max}) estimates the maximum lasing temperature depending on the excitation power. To calculate T_{SE}^{max}, we balance carrier generation and recombination to reach carrier concentration in the QW equal to the interband transparency point according to the equation,

$$\alpha_{QW} \times G_{th} = C_A \times N_{inv}^3(T_{SE}^{max}) \times f_h(T_{SE}^{max}). \quad (4)$$

The shaded area in Fig. 8 corresponds to the region where population inversion (and hence, lasing) is possible. Note that we assume carrier lifetime being determined by CCH-C AR (and so we ignore any possible contribution from concurrent Auger processes, see Fig. 1) and all optical losses (due to both free-carrier and lattice-related absorption, and also waveguide diffraction losses) being negligible; and thus, resulting T_{SE}^{max} values are, in fact, higher estimates. These T_{SE}^{max} values should be compared to effective electronic temperatures T_{eff} (dashed lines in Fig. 8 shown for several different sample temperatures), calculated as $T_{eff} \equiv T_{latt} + \delta T_e(P_{ex})$ and accounting for base (lattice) temperature T_{latt} and excitation-dependent heating term $\delta T_e(P_{ex})$ which we take from Fig. 7. We also consider $\delta T_e(P_{ex})$ being independent on the sample temperature in order to plot $T_{eff}(P_{ex})$ for different T_{latt} values in Fig. 8; and though not completely justified, it seems sufficient for approximate estimates of lasing possibility.

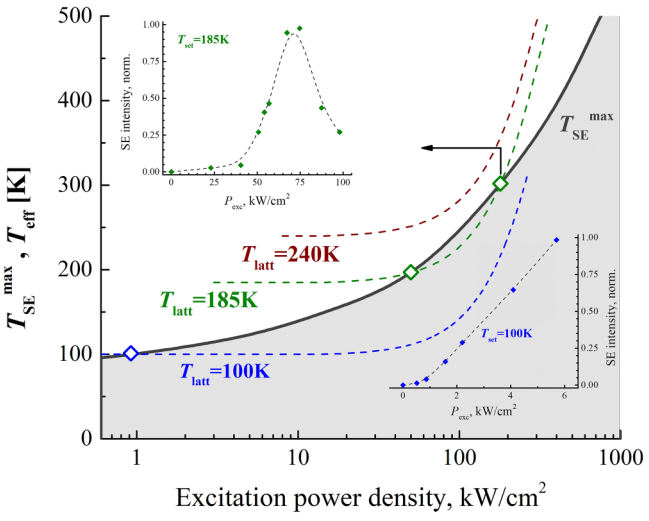

FIG. 8. Heating-induced limits for the SE from HgCdTe QWs studied in this work. Solid line (T_{SE}^{max}) represents (electronic) temperature corresponding to the QW transparency point at given excitation power; and lasing is possible below this line. Dashed lines show effective electronic temperatures depending on the excitation power. See the text for details. In the insets, excitation power dependencies of the integral SE output measured at $T = 100$ K (bottom right) and $T = 185$ K (top left).

At lower temperatures (e.g., $T = 100$ K), SE can be easily achieved with the threshold power of about 1 kW/cm^2 and it is evident from Fig. 8 that pump-induced carrier heating may not affect lasing performance under reasonable excitation. In this case plain, the linear dependence of the SE intensity on the excitation power is observed above the threshold at least up to $P_{ex} = 10 \times P_{th}$. However, at higher temperatures ($T = 185$ K in Fig. 8), there is a much smaller P_{ex} interval available to obtain SE. While at 185 K, lasing threshold P_{th} is about several tens of kW/cm^2, carrier heating sets on at some 100–150 kW/cm^2, leading to quenching of the SE at higher excitation levels (similar pump-induced SE quenching was reported earlier in Ref. 7). As a result, bell-shaped SE(P_{ex}) dependence is observed with SE onset and quenching points roughly corresponding to the pump intensities marked by diamonds in Fig. 8. Finally, at even higher temperatures ($T = 240$ K), it appears that T_{eff} always exceeds T_{SE}^{max}, and no SE could be observed. Note also that T_{eff} grows faster than T_{SE}^{max} with increasing excitation power, and so, one may not achieve lasing by any further increase in pumping intensity.

D. On the feasibility of TE-cooled operation of HgCdTe QW based mid-IR lasers

Thus, we demonstrate HgCdTe QW heterostructures with SE at 5–6 μm wavelengths observable up to $T_{max} \sim 190$–200 K which is rather close to temperatures attainable under thermoelectric cooling. While the realization of proper optical cavities (instead of single-pass amplification in this work) may provide certain advances in lasing temperatures, minimization of carrier heating feels absolutely necessary for HgCdTe QW based lasers to move further toward the room-temperature operation. Considering optically pumped structures, a direct approach to solve the problem might imply switching to an even longer excitation wavelength so that electrons and holes generated in the QWs are relatively cold and less excess energy has to be released in the QWs. However, such an approach is difficult to realize even in laboratory conditions due to weak light absorption in the QWs and lack of high-power mid-IR sources, and it is highly impractical regarding possible device applications. It also cannot be applied to electrically pumped structures since the initial energies of electrons and holes captured in the QW under injection pumping will be controlled by the barrier height. In the latter case, it is tempting to employ HgTe/CdHgTe QWs with lower barriers to reduce the amount of heat introduced in the QW and to keep effective electronic temperatures at possibly lower levels. While the realization of the highest possible band offsets, ultimately up to all-binary HgTe/CdTe QWs, was suggested in Ref. 33 to counter Auger recombination, we believe that the suppression factor for CCH-C AR is, in fact, weakly affected by the barrier height for relatively wide-gap QWs. Indeed, with a 15% decrease in [Cd] content for barrier layers (toward $Hg_{0.93}Cd_{0.07}Te/Cd_{0.45}Hg_{0.55}Te$ QWs), Auger threshold energy for the CCH-C process remains

approximately the same ($E_{th}^{*} \sim 26$ meV) as it was for 60% Cd barriers suggesting similar suppression factors for CCH-C recombination in these two cases. Based on our results, the competing CHH-H AR pathways should be of lesser concern and do not strongly affect QW design. At the same time, energy dissipated in the QW is expected to reduce nearly twofold, from ~600 (for $x[Cd]_{barr} = 60\%$) to ~300 meV ($x[Cd]_{barr} = 45\%$) per injected e–h pair. Thus, a corresponding "heating curve" (see Figs. 7 and 8) is expected to shift toward higher pumping intensities to position maximum lasing temperature comfortably into the range available for thermoelectric cooling.

Even though the feasibility of electrically pumped emitters is still questionable (appropriate p-type doping via either the introduction of mercury vacancies,[44] impurity doping,[45] or ion implantation[46] remains a major challenge for HgCdTe since all these techniques require thermal annealing which is detrimental for QW heterostructures), optically pumped HgCdTe lasers may also benefit from suggested changes in the QW design. Note that relatively high barriers in the QWs under study allow for a second electronic subband ($e2$ in Fig. 1) and so allow for another *eeh* Auger process: CCH-C2 in Fig. 1(c). While having the highest overall energy threshold ($E_{th}^{**} > 100$ meV around $T = 200$ K) among other Auger processes under discussion, this process has its energy threshold effectively split between all three interacting particles. Strong filling of the $e1$ subband by electrons necessary to achieve QW transparency at $T \sim 200$–240 K means that there is always a lot of "warm" (>30–35 meV) electrons complementing hole energy to reach the designated AR threshold. Thus, the introduction of CCH-C2 process at higher temperatures may effectively double Auger rates compared to CCH-C only, affecting both direct carrier heating by pump radiation (since more intense pumping will be required to achieve QW transparency concentration) and "indirect" carrier heating via Auger processes. At the same time, the CCH-C2 process can be eliminated in low-barrier ($x[Cd]_{barr} = 45\%$) QWs since there is only an $e1$ electronic subband present. While Auger processes similar to CCH-C2 may still exist in such QWs, these processes heat electrons into the above-barrier continuum states. In this case, we expect a much lower value for the overlap integral (due to rapidly oscillating wavefunction of the final state) and believe the related process to be weaker than "true" CCH-C2 involving all-localized states in the QW.

One final note regarding "low-barrier" QWs is that parameters of top CdHgTe layers have to be carefully balanced for optically pumped structures so that carrier generation occurs far enough from the QWs to allow efficient cooling of photoexcited carriers and these carriers still readily diffuse to the QWs to provide acceptably high pumping efficiency.

IV. SUMMARY AND CONCLUSION

To summarize, we demonstrate mid-IR stimulated emission at ~5–6 μm wavelengths from HgCdTe/CdHgTe QWs at temperatures close to 200 K. Below this critical temperature, we show that conventional CCH-C (*eeh*) type Auger recombination is a dominant interband process determining carrier lifetimes in such QWs while competing CHH-H (*ehh*) processes, including QW-specific zero-threshold Auger recombination, are supposedly weak due to strongly non-parabolic hole dispersion leading to non-trivial hole distribution function. At higher temperatures, heating of electron gas due to intense optical pumping emerges as a primary factor limiting the operation of HgCdTe QW based lasers. To minimize heating effects, we suggest implementing QWs with lower barriers (e.g., $Cd_{0.45}Hg_{0.55}Te$ instead of $Cd_{0.6}Hg_{0.4}Te$). While possibly not ideal for suppression of conventional (CCH-C) Auger recombination in HgCdTe QWs, we expect such an approach to provide the following advantages: first, smaller band offsets introduce less excess energy as carriers are trapped in the QWs, and second, elimination of excited electronic subbands inhibits respective *eeh*-type Auger processes (apart from the basic CCH-C, which appears to be only weakly affected by the barrier height). Suggested changes in the QW design may position maximum operating temperatures of mid-IR HgCdTe QW based lasers comfortably into the range accessible by thermoelectric cooling.

ACKNOWLEDGMENTS

The work was supported by the Ministry of Science and Higher Education of the Russian Federation, Grant No. 075–15-2020-797 (13.1902.21.0024). Experiments were performed using the equipment of the "Physics and technology of micro- and nanostructures" Center at IPM RAS.

AUTHOR DECLARATIONS

Conflict of Interest

The authors declare no conflict of interest.

DATA AVAILABILITY

The data that support the findings of this study are available from the corresponding author upon reasonable request.

REFERENCES

[1] A. Rogalski, "Hgcdte infrared detector material: History, status and outlook," Rep. Prog. Phys. **68**, 2267 (2005).
[2] A. Rogalski, "Next decade in infrared detectors," Proc. SPIE **10433**, 104330L (2017).
[3] J. R. Meyer, C. L. Canedy, M. Kim, C. S. Kim, C. D. Merritt, W. W. Bewley, and I. Vurgaftman, "Comparison of Auger coefficients in type I and type II quantum well midwave infrared lasers," IEEE J. Quantum Electron. **57**, 1 (2021).
[4] A. R. Beattie and P. T. Landsberg, "Auger effect in semiconductors," Proc. R. Soc. A **249**, 16 (1958).
[5] B. A. Bernevig, T. L. Hughes, and S. C. Zhang, "Quantum spin Hall effect and topological phase transition in HgTe quantum wells," Science **314**, 1757 (2006).
[6] S. A. Tarasenko, M. V. Durnev, M. O. Nestoklon, E. L. Ivchenko, J.-W. Luo, and A. Zunger, "Split Dirac cones in HgTe/CdTe quantum wells due to symmetry-enforced level anticrossing at interfaces," Phys. Rev. B **91**, 081302 (2015).
[7] S. V. Morozov, V. V. Rumyantsev, M. A. Fadeev, M. S. Zholudev, K. E. Kudryavtsev, A. V. Antonov, A. M. Kadykov, A. A. Dubinov, N. N. Mikhailov, S. A. Dvoretsky, and V. I. Gavrilenko, "Stimulated emission from HgCdTe quantum well heterostructures at wavelengths up to 19.5 μm," Appl. Phys. Lett. **111**, 192101 (2017).
[8] J. Bleuse, N. Magnea, L. Ulmer, J. L. Pautrat, and H. Mariette, "Room-temperature laser emission near 2 μm from an optically pumped HgCdTe separate-confinement heterostructure," J. Cryst. Growth **117**, 1046 (1992).

[9]J. Bleuse, J. Bonnet-Gamard, G. Mula, N. Magnea, and P. Jean-Louis, "Laser emission in HgCdTe in the 2–3.5 μm range," J. Cryst. Growth **197**, 529 (1999).
[10]A. A. Andronov, Y. N. Nozdrin, A. V. Okomel'kov, N. N. Mikhailov, G. Y. Sidorov, and V. S. Varavin, "Stimulated emission from optically excited $Cd_xHg_{1-x}Te$ structures at room temperature," J. Lumin. **132**, 612 (2012).
[11]C. Roux, E. Hadji, and J.-L. Pautrat, "Room-temperature optically pumped CdHgTe vertical-cavity surface-emitting laser for the 1.5 μm range," Appl. Phys. Lett. **75**, 1661 (1999).
[12]M. A. Fadeev, A. O. Troshkin, A. A. Dubinov, V. V. Utochkin, A. A. Razova, V. V. Rumyantsev, V. Y. Aleshkin, V. I. Gavrilenko, N. N. Mikhailov, S. A. Dvoretsky, and S. V. Morozov, "Mid-infrared stimulated emission in HgCdTe/CdHgTe quantum well heterostructures at room temperature," Opt. Eng. **60**, 082006 (2021).
[13]E. Tournié and A. N. Baranov, "Mid-infrared semiconductor lasers: A review," Semicond. Semimetals **86**, 183 (2012).
[14]L. Cerutti, A. Vicet, and E. Tournie, *Interband Mid-Infrared Lasers. Mid-Infrared Optoelectronics Materials, Devices, and Applications* (Woodhead Publishing Series in Electronic and Optical Materials, 2020), pp. 91–130.
[15]A. Ishida and S. Nakashima, "PbSrS/PbS mid-infrared short-cavity edge-emitting laser on Si substrate," Appl. Phys. Lett. **111**, 161104 (2017).
[16]M. S. Vitiello, G. Scalari, B. Williams, and P. de Natale, "Quantum cascade lasers: 20 years of challenges," Opt. Express **23**, 5167 (2015).
[17]J. R. Meyer, W. W. Bewley, C. L. Canedy, C. S. Kim, M. Kim, C. D. Merritt, and I. Vurgaftman, "The interband cascade laser," Photonics **7**, 75 (2020).
[18]J. P. Zanatta, F. Noël, P. Ballet, N. Hdadach, A. Million, G. Destefanis, E. Mottin, C. Kopp, E. Picard, and E. Hadji, "HgCdTe molecular beam epitaxy material for microcavity light emitters: Application to gas detection in the 2–6 μm range," J. Electron. Mater. **32**, 602 (2003).
[19]M. A. Fadeev, V. V. Rumyantsev, A. M. Kadykov, A. A. Dubinov, A. V. Antonov, K. E. Kudryavtsev, S. A. Dvoretskii, N. N. Mikhailov, V. I. Gavrilenko, and S. V. Morozov, "Stimulated emission in the 2.8–3.5 μm wavelength range from Peltier cooled HgTe/CdHgTe quantum well heterostructures," Opt. Express **26**(10), 12755 (2018).
[20]V. Rumyantsev, M. Fadeev, V. Aleshkin, N. Kulikov, V. Utochkin, N. Mikhailov, S. Dvoretskii, S. Pavlov, H.-W. Hübers, V. Gavrilenko, C. Sirtori, Z. F. Krasilnik, and S. Morozov, "Carrier recombination, long-wavelength photoluminescence and stimulated emission in HgCdTe quantum well heterostructures," Phys. Status Solidi B **256**, 1800546 (2019).
[21]V. V. Utochkin, K. E. Kudryavtsev, M. A. Fadeev, A. A. Razova, D. S. Bykov, V. Ya Aleshkin, A. A. Dubinov, N. N. Mikhailov, S. A. Dvoretsky, V. V. Rumyantsev, V. I. Gavrilenko, and S. V. Morozov, "Mid-IR stimulated emission in Hg(Cd)Te/CdHgTe quantum well structures up to 200 K due to suppressed Auger recombination," Laser Phys. **31**, 015801 (2021).
[22]J. M. Arias, M. Zandian, R. Zucca, and J. Singh, "Hgcdte infrared diode lasers grown by MBE," Semicond. Sci. Technol. **8**, S255 (1993).
[23]F. Bartoli, R. Allen, L. Esterowitz, and M. Kruer, "Auger-limited carrier lifetimes in HgCdTe at high excess carrier concentrations," J. Appl. Phys. **45**, 2150 (1974).
[24]K. Jóźwikowski, M. Kopytko, and A. Rogalski, "The bulk generation-recombination processes and the carrier lifetime in midwave infrared and long-wave infrared liquid nitrogen cooled HgCdTe alloys," J. Appl. Phys. **112**, 033718 (2012).
[25]H. Wen, B. Pinkie, and E. Bellotti, "Direct and phonon-assisted indirect Auger and radiative recombination lifetime in HgCdTe, InAsSb, and InGaAs computed using Green's function formalism," J. Appl. Phys. **118**, 015702 (2015).
[26]C. M. Ciesla, B. N. Murdin, T. J. Phillips, A. M. White, A. R. Beattie, C. J. G. M. Langerak, C. T. Elliott, and C. R. Pidgeon, "Auger recombination dynamics in highly excited HgCdTe," Phys. Status Solidi B **204**, 121 (1997).
[27]S. V. Morozov, M. S. Joludev, A. V. Antonov, V. V. Rumyantsev, V. I. Gavrilenko, V. Y. Aleshkin, A. A. Dubinov, N. N. Mikhailov, S. A. Dvoretskiy, O. Drachenko, S. Winnerl, H. Schneider, and M. Helm, "Study of lifetimes and photoconductivity relaxation in heterostructures with $Hg_xCd_{1-x}Te/Cd_yHg_{1-y}Te$ quantum wells," Semiconductors **46**, 1362 (2012).
[28]S. Ruffenach, A. Kadykov, V. V. Rumyantsev, J. Torres, D. Coquillat, D. But, S. S. Krishtopenko, C. Consejo, W. Knap, S. Winnerl, M. Helm, M. A. Fadeev, N. N. Mikhailov, S. A. Dvoretskii, V. I. Gavrilenko, S. V. Morozov, and F. Teppe, "HgCdTe-based heterostructures for terahertz photonics," APL Mater. **5**, 035503 (2017).
[29]K. E. Kudryavtsev, V. V. Rumyantsev, V. Y. Aleshkin, A. A. Dubinov, V. V. Utochkin, M. A. Fadeev, N. N. Mikhailov, G. Alymov, D. Svintsov, V. I. Gavrilenko, and S. V. Morozov, "Temperature limitations for stimulated emission in 3–4 μm range due to threshold and non-threshold Auger recombination in HgTe/CdHgTe quantum wells," Appl. Phys. Lett. **117**, 083103 (2020).
[30]C. H. Grein, P. M. Young, and H. Ehrenreich, "Minority carrier lifetimes in ideal InGaSb/InAs superlattices," Appl. Phys. Lett. **61**, 2905 (1992).
[31]M. Asada, A. Kameyama, and Y. Suematsu, "Gain and intervalence band absorption in quantum-well lasers," IEEE J. Quantum Electron. **20**, 745 (1984).
[32]M. E. Flatté, C. H. Grein, H. Ehrenreich, R. H. Miles, and H. Cruz, "Theoretical performance limits of 2.1–4.1 μm InAs/InGaSb, HgCdTe, and InGaAsSb lasers," J. Appl. Phys. **78**, 4552 (1995).
[33]I. Vurgaftman and J. R. Meyer, "High-temperature HgTe/CdTe multiple-quantum-well lasers," Opt. Express **2**, 137 (1998).
[34]I. Vurgaftman, J. R. Meyer, J. M. Dell, T. A. Fisher, and L. Faraone, "Simulation of mid-infrared HgTe/CdTe quantum-well vertical-cavity surface emitting lasers," J. Appl. Phys. **83**, 4286 (1998).
[35]N. N. Mikhailov, R. N. Smirnov, S. A. Dvoretsky, Y. G. Sidorov, V. A. Shvets, E. V. Spesivtsev, and S. V. Rykhlitski, "Growth of $Hg_{1-x}Cd_xTe$ nanostructures by molecular beam epitaxy with ellipsometric control," Int. J. Nanotechnol. **3**, 120 (2006).
[36]S. Dvoretsky, N. Mikhailov, Y. Sidorov, V. Shvets, S. Danilov, B. Wittman, and S. Ganichev, "Growth of HgTe quantum wells for IR to THz detectors," J. Electron. Mater. **39**, 918 (2010).
[37]G. Alymov, V. Rumyantsev, S. Morozov, V. Gavrilenko, V. Aleshkin, and D. Svintsov, "Fundamental limits to far-infrared lasing in Auger-suppressed HgCdTe quantum wells," ACS Photonics **7**, 98 (2020).
[38]M. Zholudev, F. Teppe, M. Orlita, C. Consejo, J. Torres, N. Dyakonova, M. Czapkiewicz, J. Wróbel, G. Grabecki, N. Mikhailov, S. Dvoretskii, A. Ikonnikov, K. Spirin, V. Aleshkin, V. Gavrilenko, and W. Knap, "Magnetospectroscopy of two-dimensional HgTe-based topological insulators around the critical thickness," Phys. Rev. B **86**, 205420 (2012).
[39]G. M. Minkov, V. Y. Aleshkin, O. E. Rut, A. A. Sherstobitov, A. V. Germanenko, S. A. Dvoretski, and N. N. Mikhailov, "Electron mass in a HgTe quantum well: Experiment versus theory," Physica E **116**, 113742 (2020).
[40]J. Polit, "Model of the two well potential for Hg-atoms in the $Hg_{1-x}Cd_xTe$ alloy lattice," Bull. Pol. Acad. Sci. Tech. Sci. **59**, 331 (2011).
[41]C. H. Grein, M. E. Flatté, and Y. Chang, "Modeling of recombination in HgCdTe," J. Electron. Mater. **37**, 1415 (2008).
[42]V. Y. Aleshkin, V. V. Rumyantsev, K. E. Kudryavtsev, A. A. Dubinov, V. V. Utochkin, M. A. Fadeev, G. Alymov, N. N. Mikhailov, S. A. Dvoretsky, F. Teppe, V. I. Gavrilenko, and S. V. Morozov, J. Appl. Phys. **129**, 133106 (2021).
[43]V. Y. Aleshkin, A. A. Dubinov, V. V. Rumyantsev, and S. V. Morozov, "Threshold energies of Auger recombination in HgTe/CdHgTe quantum well heterostructures with 30–70 meV bandgap," J. Phys. Condens. Matter **31**, 425301 (2019).
[44]J. Garland, "Chap. 7: MBE growth of mercury cadmium telluride," in *Mercury Cadmium Telluride: Growth, Properties and Applications*, edited by P. Capper and J. W. Garland (John Wiley & Sons Ltd., West Sussex, 2011), pp. 131–149.
[45]M. Zandian, A. C. Chen, D. D. Edwall, J. G. Pasko, and J. M. Arias, "*p*-type arsenic doping of $Hg_{1-x}Cd_xTe$ by molecular beam epitaxy," Appl. Phys. Lett. **71**, 2815 (1997).
[46]V. M. Bazovkin, S. A. Dvoretsky, A. A. Guzev, A. P. Kovchavtsev, D. V. Marin, V. G. Polovinkin, I. V. Sabinina, G. Y. Sidorov, A. V. Tsarenko, V. V. Vasil'ev, V. S. Varavin, and M. V. Yakushev, "High operating temperature SWIR p^+–n FPA based on MBE-grown HgCdTe/Si(013)," Infrared Phys. Technol. **76**, 72 (2016).